GEOLOGY | THE GEOLOGICAL SOCIETY OF AMERICA®

https://doi.org/10.1130/G50998.1

Manuscript received 12 August 2022
Revised manuscript received 28 March 2023
Manuscript accepted 18 April 2023

Published online 8 May 2023

Fast exhumation of Earth's earliest ultrahigh-pressure rocks in the West Gondwana orogen, Mali

Carlos E. Ganade[1,2,*], Daniela Rubatto[2], Pierre Lanari[2], Joerg Hermann[2], Lucas R. Tesser[3], and Renaud Caby[4]
[1]Center of Applied Geosciences (CGA), Geological Survey of Brazil, 22290-255 Rio de Janeiro, Brazil
[2]Institut für Geologie, Universität Bern, 3012 Bern, Switzerland
[3]Institute of Geosciences, University of São Paulo, 05508-080 São Paulo, Brazil
[4]Géosciences Montpellier, Université de Montpellier II, Montpellier CEDEX 5, France

ABSTRACT

Did exhumation of ultrahigh-pressure (UHP) rocks proceed at comparable rates in the Neoproterozoic and in modern collisional orogens? We address this question with a multi-mineral geochronological study of UHP rocks from the Gourma fold-and-thrust belt in Mali. Integrated petrology and zircon U-Pb geochronology reveal peak metamorphic conditions of 820–740 °C and 3.3–3.4 GPa at 611.7 ± 3.6 Ma, providing evidence for subduction of the passive margin of the West African craton to ~125 km depth in the West Gondwana orogen. Rutile U-Pb cooling ages indicate further exhumation of the Gourma UHP unit to mid-crustal levels (~35 km) at 601.7 ± 3.2 Ma. These two ages provide a time lag between peak conditions and exhumation to 35 km of 10 ± 3.1 m.y., constraining an average vertical exhumation rate of 0.9 ± 0.3 cm/yr. Our data indicate a fast exhumation rate for the oldest known UHP rocks, comparable to that reported for modern collisional orogens. We argue that exhumation of the deeply subducted UHP rocks along the West Gondwana orogen contributed to significant changes in the Neoproterozoic atmosphere and biosphere.

INTRODUCTION

The emergence of modern-style mechanisms for plate tectonics is one of the most debated issues in the geological literature (Cawood et al., 2018), but direct evidence for deep continental subduction at ultrahigh-pressure (UHP) conditions in the geological record is limited to Neoproterozoic and younger times (Stern, 2018). The transport of continental rocks to UHP conditions equivalent to depths >100 km, where coesite is stable (Chopin, 1984; Smith, 1984), and their exhumation back to mid-crustal levels is a common process in Phanerozoic collisional orogens such as the Alps and Himalayas. Coesite-bearing rocks from the Gourma fold-and-thrust belt (Caby, 1994) of the West Gondwana orogen represent the oldest unambiguous record of UHP rocks (Jahn et al., 2001; Ganade et al., 2014). In this belt, burial to UHP conditions at ca. 610 Ma has been previously defined (Caby, 1994; Ganade et al., 2014), however the detailed pressure-temperature-time (*P-T-t*) trajectory of these rocks during continental subduction and exhumation remains unconstrained. This period also coincides with critical changes in the Earth's atmosphere and biosphere, leading to the hypothesis that these changes were triggered in part by the growth and erosion of Himalayan-sized mountains (Squire et al., 2006; Campbell and Allen, 2008; Ganade et al., 2014).

Here, we report a petrochronological investigation that unravels the exhumation rate of these important UHP rocks. Our results define a fast exhumation rate for these earliest UHP rocks, suggesting that the process of exhumation has similar constraints to those recorded in the Phanerozoic collisional orogens. We suggest here that the interdependence of low latitude, tectonics, and climatically driven erosion may have influenced critical changes in the Neoproterozoic atmosphere and biosphere.

THE GOURMA FOLD-AND-THRUST BELT (WEST GONDWANA OROGEN)

The Gourma fold-and-thrust belt of northern Mali hosts UHP coesite-bearing rocks (Caby, 1994) and is part of the >2500-km-long orogen that resulted from the closure of the Goiás-Pharusian Ocean (Caby, 1989; Ganade et al., 2014). The orogen culminated in a continent-continent collision, mainly involving the conjoined Amazon and West African cratons against the São Francisco–Congo and Saharan cratons (Fig. 1A). Subduction was long lived (>400 m.y.), resulting in the development of several intra-oceanic and continental arcs that are now partially preserved within a deeply eroded paleo-collisional zone (Caby, 1989; Ganade et al., 2014, 2021). The collisional period has been defined by U-Pb dating of UHP eclogitic zircons along the orogen in Brazil, Togo, and Mali and can be bracketed between 615 and 610 Ma (Ganade et al., 2014). The erosion of mountains resulting from the collision is documented in syn- to post-collisional sedimentary deposits, and the termination of orogenic activity is dated by the age of post-collisional granitoids ranging from 580 to 520 Ma (Liégeois and Black, 1987; Ganade et al., 2014).

The rock assemblage of the Gourma fold-and-thrust belt represents the subducted, rifted passive continental margin of the West African craton (Caby, 1989). It consists of shelf carbonates grading eastward to turbiditic slope facies overlain by a thick terrigenous turbidite sequence (Caby, 1979; Jahn et al., 2001). The proximal portion of the passive margin consists of folded low-grade metasedimentary rocks and undeformed strata of the Ydouban and Hombori formations, respectively (Fig. 1B) (Reichelt, 1966; Caby, 1979). The inner part of the margin has been affected by collisional tectonics that imprinted a westward vergence toward the West African craton. This inner part consists of greenschist facies rocks of the external nappes (Adouf turbidites) and high-pressure nappes that include eclogites and garnet blueschists around Assongo (Caby et al., 2008) (Fig. 1B).

Carlos Ganade https://orcid.org/0000-0002-2896-0551
*carlos.ganade@cprm.gov.br

CITATION: Ganade, C.E., et al., 2023, Fast exhumation of Earth's earliest ultrahigh-pressure rocks in the West Gondwana orogen, Mali: Geology, v. 51, p. 647–651, https://doi.org/10.1130/G50998.1

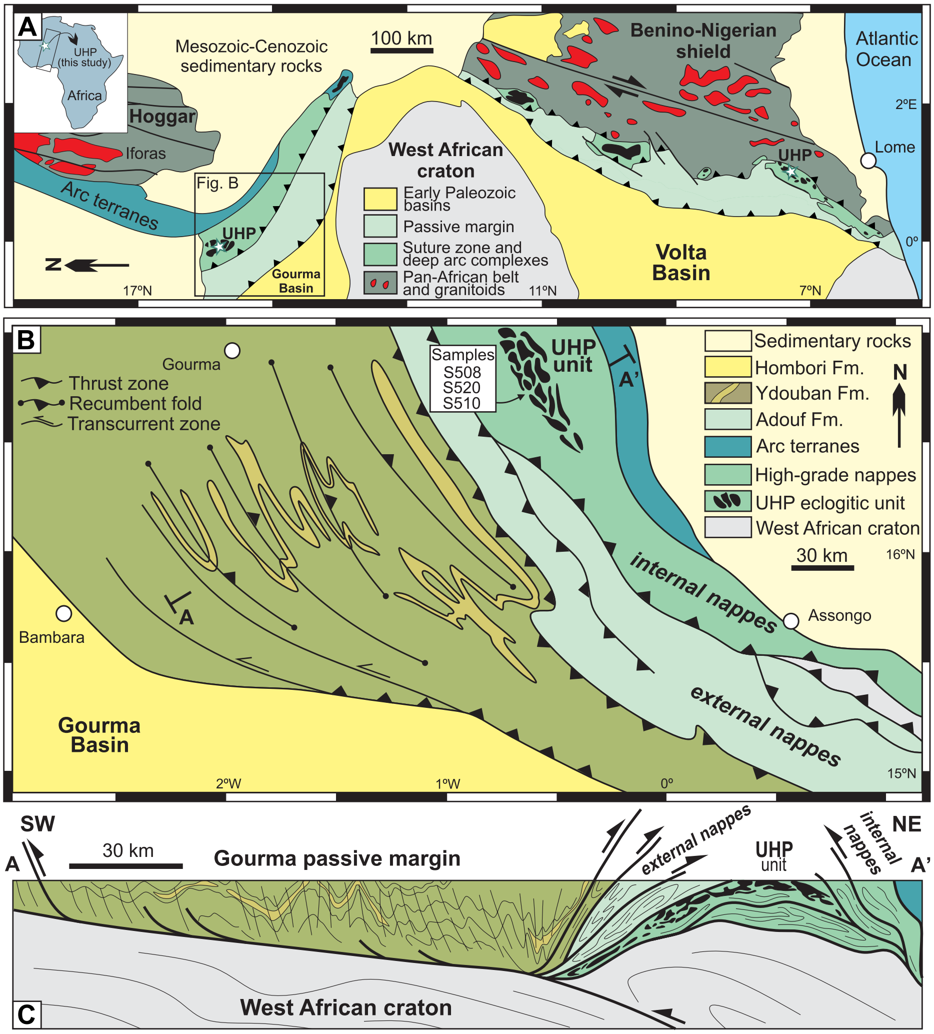

Figure 1. Geological context of the West African craton and Gourma fold-and-thrust belt. (A) Continental-scale geological context of the West Gondwana orogen in Africa (Ganade et al., 2014). (B) Geological map of the Gourma fold-and-thrust belt. (C) Cross section of the Gourma region after Caby (1989). UHP—ultrahigh pressure.

This ~10,000 km² unit preserves high-pressure metamorphic assemblages represented by phengite-garnet-omphacite-rutile assemblages and kyanite in aluminous quartzites, including a 3-km-thick imbricated flat-lying UHP eclogitic unit, the source of the samples investigated here.

PETROLOGY AND DATING OF ACCESSORY PHASES

Petrological investigations combined with time-stamped zircon trace element and rutile U-Pb geochronology were used to constrain the *P-T-t* history of the UHP eclogitic Gourma terrane. Two impure quartzite samples (S508 and S520) and one eclogite sample (S510) were collected in the region of In Edem within the coesite-bearing UHP domain (Caby, 1994). Thin sections were mapped with an electron probe micro-analyzer to determine mineral compositional zoning (Lanari et al., 2014) and for *P-T* modeling combined with U-Pb geochronology and trace elements of zircon and rutile. Analytical procedures and detailed results are provided in the Supplemental Material[1].

Element maps for samples S508 and S520 show a peak metamorphic assemblage of garnet-omphacite-phengite-kyanite-coesite-(quartz)-rutile with retrograde amphibole, paragonite, epidote, albite, and chlorite (Figs. 2A and 2B). Sample S510 has an inferred peak metamorphic assemblage of garnet-omphacite-(quartz)-coesite-rutile and retrograde amphibole, epidote, and paragonite (Fig. 2C).

The topology of the phase equilibrium diagrams for the samples from the internal nappe sequence are similar (Fig. 2; Fig. S1 in the Supplemental Material), with low-variance fields bounding the stability field of garnet-omphacite-phengite-bearing assemblages at temperatures above 650–700 °C and pressures between 2.0 and 3.5 GPa. In general, the transition from high- to low-pressure equilibrium fields is accompanied by an increase in amphibole and epidote volume at the expense of garnet and omphacite. In all models, the calculated peak metamorphic assemblages are high-variance fields (variance $v = 4$ or 5). The combined isopleth intercept area of high-Si per formula unit (pfu) in phengite, jadeite molecule in omphacite (X_{Jd}), and grossular molecule in garnet (X_{Grs}) indicates similar average peak metamorphic conditions for the metasedimentary rocks of 3.36 ± 0.16 GPa and 743 ± 44 °C (sample S508) and 3.46 ± 0.14 GPa and 825 ± 34 °C (sample 520). For the eclogite sample S510, the interception of the isopltehs of X_{Jd} in omphacite and pyrope molecule (X_{Prp}) in garnet yielded a less-constrained *P-T* conditions of 2.66 ± 0.31 GPa and 725 ± 57 °C.

Metamorphic zircon in both eclogite and quartzite is represented by overgrowths around ca. 900 Ma cores (Data Set S1 in the Supplemental Material) and structureless to sector-zoned rounded crystals (Fig. 3A) with omphacite and garnet inclusions (Fig. S2). Zircon cores and rims and structureless crystals were dated with secondary ionization mass spectrometry (SIMS; methods in Supplemental Material). For eclogite S510, zircon dates from nine round structureless zircon crystals and zircon rims define a concordia age of 610.3 ± 4.7 Ma (2σ, MSWD = 1.00) (Fig. 3B). Metamorphic zircon overgrowths from the UHP quartzite S508 define a concordia age of 613.9 ± 5.8 Ma (2σ, MSWD = 0.29) (Fig. 3B). Because both samples were collected from the same structural level at the same location within the In Edem well and have the same zircon texture and chemistry, both ages can be combined to define a concordia age of 611.7 ± 3.6 Ma (2σ, MSWD = 0.57) (Fig. 3B). In both samples, metamorphic zircon is characterized by a flat heavy rare earth element pattern and the absence of a pronounced Eu anomaly (Fig. 3), indicating that, in contrast to the older cores, they grew in the presence of garnet and in the absence of plagioclase (e.g., Rubatto, 2002, 2017). Titanium contents for the metamorphic zircons from eclogite S510 and impure quartzite S508 range from 7.2 to 17.6 ppm and 7.3 to 24.5 ppm, respectively, resulting in Ti-in-zircon temperatures (Watson et al., 2006) of 746 ± 23 °C and 795 ± 21, respectively (Data Set S1; Fig. 3A).

Rutile grains with equatorial areas ranging in size from 10 to 50 mm² from UHP kyanite-bearing quartzite (samples S508 and S520) were dated by laser ablation–inductively coupled plasma–mass spectrometry (LA-ICP-MS). A regression based on 20 spot analyses in rutile grains from sample S508 yield a mean $^{206}Pb/^{238}U$ date of 608.1 ± 4.9 Ma (2σ, MSWD = 2.3) with an initial $^{207}Pb/^{206}Pb$ intercept at 0.89 ± 0.02. For

[1]Supplemental Material. Analytical procedures and detailed petrology. Please visit https://doi.org/10.1130/GEOL.S.22688005 to access the supplemental material, and contact editing@geosociety.org with any questions.

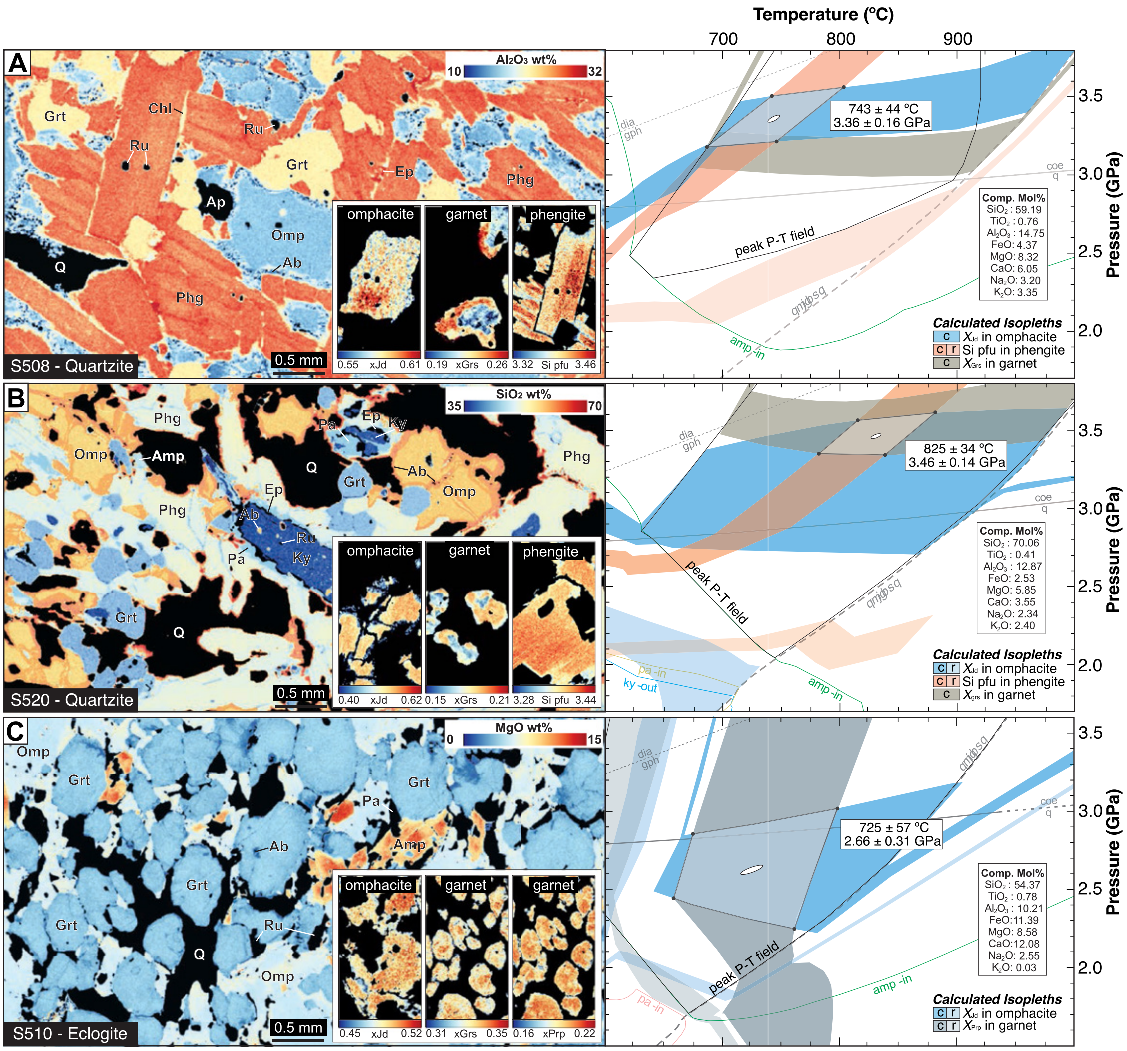

Figure 2. Mineral distribution (left) and compositional variation of garnet, omphacite, and phengite together with isopleth thermobarometric results (right). (A) Quartzite sample S508. (B) Quartzite sample S520. (C) Eclogite sample S510. Pfu—per formula unit; X_{Jd}—jadeite molecule; X_{Grs}—grossular molecule; X_{Prp}—pyrope molecule; Grt—garnet; Omp—omphacite; Phg—phengite; Ky—kyanite; Rt—rutile; Pa—paragonite; Amp—amphibole; Ep—epidote; Ab—albite; Chl—chlorite; Ap—apatite; Q—quartz; Coe—coesite; Gph—graphite; Dia—diamond.

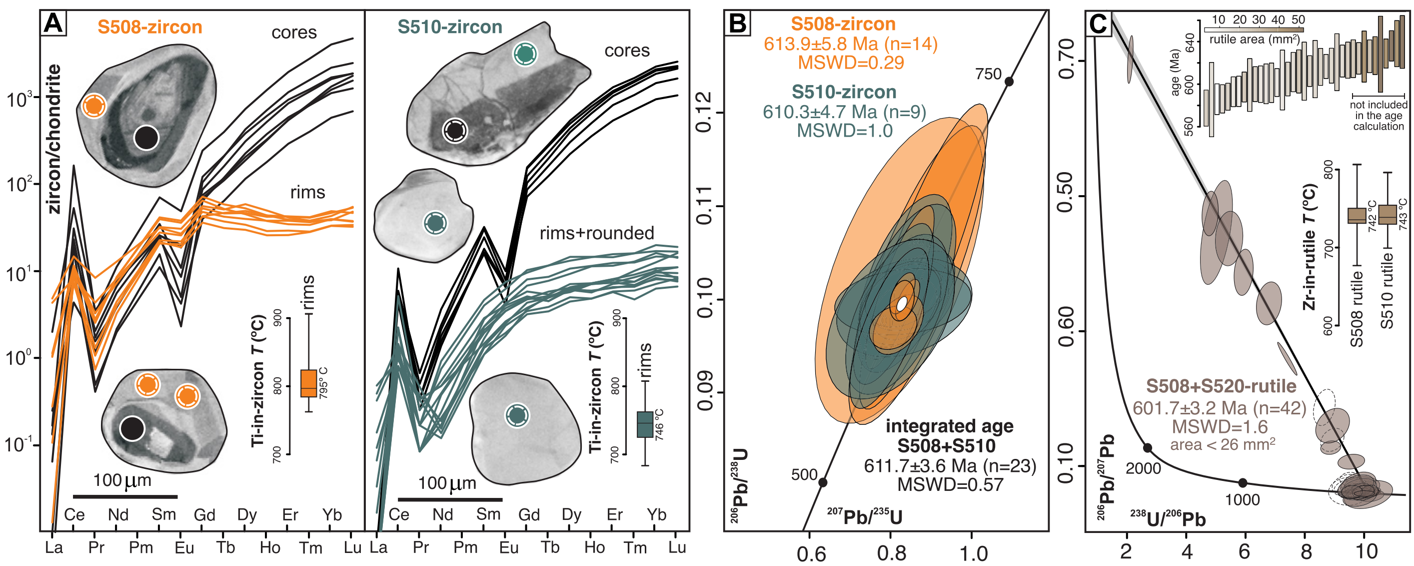

Figure 3. Zircon geochronology and trace elements. (A) Internal zircon structure and rare earth element (REE) composition for samples S508 and S510. Spots refer to REE analyses in the zircon core (black) and metamorphic rims and rounded zircons (orange and green). Dashed smaller spot refers to U-Pb analyses. (B) Wetherill concordia plots of U-Pb zircon data from samples S508 (orange) and S510 (green). (C) U-Pb Tera-Wasserburg plot for rutile grains from quartzite samples S508 and S520. Dashed ellipses refer to rutile grains with an equatorial area >26 mm² and are not included in the age calculation. MSWD—mean square of weighted deviates.

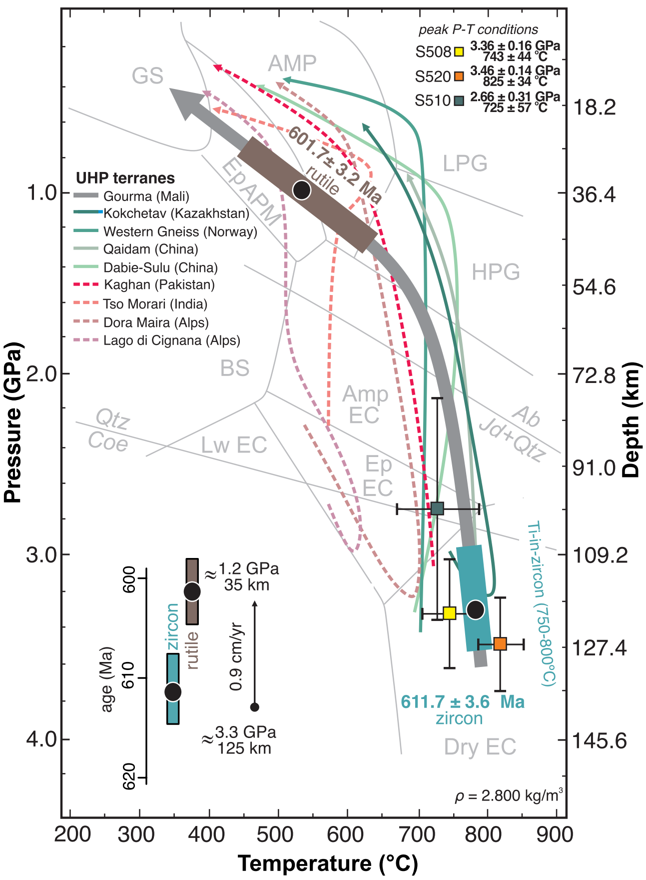

Figure 4. Integrated pressure-temperature-time (*P-T-t*) trajectory of the Gourma ultrahigh-pressure (UHP) terrane. *P-T* trajectories extracted from Kylander-Clark et al. (2012) from other small (dashed lines) and large (solid lines). UHP terranes worldwide are shown for comparison. Lower-left inset illustrates vertical exhumation rate based on 2σ uncertainty of the U-Pb geochronology data of zircon and rutile. Metamorphic facies: GS—green schist; AMP—amphibolite; LPG—low-pressure granulite; HPG—high-pressure granulite; BS—blue schist; EC—eclogite; Ep—epidote; Amp—amphibolite; Lw—lawsonite, Ab—albite; Jd—jadeite; Qtz—quartz; Coe—coesite.

sample S520, an isochron of 29 spot analyses yielded a mean date of 602.8 ± 4.1 Ma (2σ, MSWD = 1.9) with initial $^{207}Pb/^{206}Pb$ intercept of 0.87 ± 0.19. Individual rutile dates are correlated with grain area, with smaller grains tending to be younger, indicating that rutile dates are controlled by diffusion (Fig. 3C). Given the comparable initial $^{207}Pb/^{206}Pb$ and the proximity of the two samples, a cumulative age considering only the smallest grains is calculated at 601.7 ± 3.2 Ma (2σ, MSWD = 1.6) (Fig. 3C). Zirconium concentrations in rutile from samples S508 and S510 are similar, ranging from 120 to 535 ppm and yielding mean Zr-in-rutile temperatures (Watson et al., 2006) of 742 ± 30 °C and 743 ± 25 °C, respectively (Data Set S2). Zirconium diffusion in rutile is significantly slower than that of Pb and robust to high temperature (Cherniak et al., 2007; Ewing et al., 2013), so Zr-in-rutile temperatures are interpreted as formation temperatures and predate the cooling ages.

DISCUSSION: PACE OF EXHUMATION OF EARLIEST UHP ROCKS

Phase equilibrium modeling and isopleth thermobarometry for the Gourma UHP rocks support metamorphic conditions in the coesite stability field with pressures between 3.4 and 3.3 GPa. Together with evidence for coesite (Caby, 1994), such peak conditions provide an unambiguous record of subduction of the West African craton passive margin to UHP at 820–740 °C with an apparent geothermal gradient of 240–220 °C/GPa. Trace element composition and mineral inclusions in metamorphic zircon from samples S510 and S508 indicate zircon growth at eclogitic conditions. Average Ti-in-zircon thermometry (Watson et al., 2006) of metamorphic overgrowths returns temperatures of 800–750 °C, within the uncertainty of temperatures from thermobarometry results. Therefore, we interpret the zircon age of 611.7 ± 3.6 Ma (2σ) to mark the transition from the peak to the onset of exhumation in the studied rocks (Fig. 4).

Retrograde textures and minerals such as symplectic intergrowth of clinopyroxene, amphibole, albite, and quartz after Na-rich omphacite, and paragonite growth after kyanite, indicate decompression from 3.4 GPa to 1.6 GPa accompanied by cooling from 820–740 °C to 620–650 °C. The appearance of epidote during retrogression suggests yet further decompression and cooling to 1.0 GPa and 500 °C (Fig. 4). Rutile is clearly stable during peak conditions as documented by the textures and Zr-in-rutile temperatures. However, the correlation of rutile size with the concordant U-Pb dates and the younger age compared to eclogitic zircon suggest that Pb diffusion was active after the formation of rutile. Therefore, the U-Pb dates of these grains correspond to the cooling age rather than the formation age of the rutile grains. Closure temperatures for Pb diffusion have been estimated at ~600 °C (Cherniak, 2000) and 550–450 °C (Kooijman et al., 2010) for rutile grains of ~100 μm, and decoupling of Zr-in-rutile temperatures from U-Pb ages is commonly observed in high-grade rutile (Ewing et al., 2015). Taking the interval for the closure temperature of Pb in rutile of 600–450 °C together with the proposed *P-T* trajectory, the 601.7 ± 3.2 Ma (2σ) age obtained from the smallest rutile grains is attributed to cooling at ~1.2 GPa. The zircon age of 611.7 ± 3.6 Ma at the transition from the peak to the onset of exhumation at ~3.3 GPa and the rutile cooling age provide a time interval of 10 ± 3.1 m.y. for vertical exhumation from 125 to 35 km depth (assuming an average density of 2800 kg/m³ for the rock column). This interval implies a fast vertical exhumation rate of 0.9 ± 0.3 cm/yr.

Exhumation of UHP rocks has been described as a two-stage process (e.g., Duchêne et al., 1997). Aided by tectonic forces, buoyancy has been suggested to be the main driving force for exhumation of deeply subducted continental crust to 40–30 km depth in a balance between down-channel shear traction and up-channel buoyancy (Ernst et al., 1997; Warren et al., 2008). The average vertical exhumation rates from peak UHP conditions to 40 km depth of 13 selected Phanerozoic collisional orogens are fast at ~1.9 cm/yr (Yan and Zhang, 2019), with the fastest exhumation rates of 3–8 cm/yr reported for the Dora Maira (Western Alps), Kokchetav Massif (Kazakhstan), and Kaghan Valley (Pakistan) terranes (Hermann et al., 2001; Rubatto and Hermann, 2001; Parrish et al., 2006). Our estimate for the rapid vertical exhumation of the Gourma UHP unit to mid-crustal levels (~40 km) suggests similar tectonic processes and conditions to those of modern collision in the late Neoproterozoic.

Exhumation from 40–45 km to the surface is generally associated with climate-driven erosion at low latitudes (Yan and Zhang, 2019), which can directly influence tectonic deformation in collisional zones (Beaumont et al., 1991). Paleomagnetic data indicate that the formation of the 2500-km-long West Gondwana orogen occurred at low latitudes (2.2°N–16.8°N) during an interglacial period (Yan and Zhang, 2019). We argue that the Marinoan deglaciation may have been enhanced by an increase in atmospheric CO_2 sourced from the extensive arc magmatism from 650 to 620 Ma that preceded the continental collision (e.g., Ganade et al., 2021; Sun et al., 2022). Exhumation of deeply subducted rocks along the West Gondwana orogen to the surface due to precipitation, rapid erosion, and active faulting may have contributed to the increase in $^{87}Sr/^{86}Sr$ in the oceans (Halverson et al., 2007) and the net decrease in atmospheric CO_2 due to enhanced silicate weathering that occurred at ca. 600 Ma. As a result, nutrient-rich rivers dissecting the West Gondwana orogen fertilized the shelf area, paving the way for the Ediacaran expansion of metazoan ecosystems (Ganade et al., 2014), and may have triggered the minor Gaskier glaciation at ca. 580 Ma.

CONCLUSIONS

Zircon and rutile U-Pb ages and petrology for the oldest known coesite-bearing UHP rocks from the Gourma fold-and-thrust belt, Mali, constrain a vertical exhumation rate from 125–35 km depth of 0.9 ± 0.3 cm/yr for the subducted passive margin of the West African craton. This value is in agreement with those reported for Phanerozoic collisional orogens, suggesting that the conditions for the operation of modern collisional orogens were already present during the late Neoproterozoic. Due to its low-latitude position, we suggest that the exhumation of this large unit from 40 km to the surface may have been climatically driven and that enhanced weathering and erosion affected both the Neoproterozoic atmosphere and biosphere.

ACKNOWLEDGMENTS

This research was supported by the Serrapilheira Institute (Serra–1709-21887), Swiss National Science Foundation Project N IZESO_l94628, and the Geological Survey of Brazil. We thank R.F. Weinberg for the suggestions in the early version of the manuscript and F. Piccoli for assistance with LA-ICP-MS analyses of rutile. C. Warren, S. Guillot, and an anonymous reviewer are thanked for the suggestions in an earlier version of the manuscript.

REFERENCES CITED

Beaumont, C., Fulsack, P., and Hamilton, J., 1991, Erosional control of active compressional orogens, *in* McClay, K.R., ed., Thrust Tectonics: New York, Chapman and Hall, p. 1–18.

Caby, R., 1979, Les nappes précambriennes du Gourma dans la chaîne panafricaine du Mali: Comparaison avec les Alpes occidentales: Revue de Géologie Dynamique et de Géographie Physique, v. 21, p. 365–376.

Caby, R., 1989, Precambrian terranes of Benin-Nigeria and northeast Brazil and the Late Proterozoic south Atlantic fit, *in* Dallmeyer, R.G., ed., Terranes in the Circum-Atlantic Paleozoic Orogens: Geological Society of America Special Paper 230, p. 145–158, https://doi.org/10.1130/SPE230-p145.

Caby, R., 1994, Precambrian coesite from northern Mali: First record and implications for plate tectonics in the trans-Saharan segment of the Pan-African belt: European Journal of Mineralogy, v. 6, p. 235–244, https://doi.org/10.1127/ejm/6/2/0235.

Caby, R., Buscail, F., Dembélé, D., Diakité, S., Sacko, S., and Bal, M., 2008, Neoproterozoic garnet-glaucophanites and eclogites: New insights for subduction metamorphism of the Gourma fold and thrust belt (eastern Mali), *in* Ennih, N., and Liégeois, J.-P., eds., The Boundaries of the West African Craton: Geological Society, London, Special Publication 297, p. 203–216, https://doi.org/10.1144/SP297.9.

Campbell, I.H., and Allen, C.M., 2008, Formation of supercontinents linked to increases in atmospheric oxygen: Nature Geoscience, v. 1, p. 554–558, https://doi.org/10.1038/ngeo259.

Cawood, P.A., Hawkesworth, C.J., Pisarevsky, S.A., Dhuime, B., Capitanio, F.A., and Nebel, O., 2018, Geological archive of the onset of plate tectonics: Philosophical Transactions of the Royal Society A: Mathematical, Physical and Engineering Sciences, v. 376, https://doi.org/10.1098/rsta.2017.0405.

Cherniak, D.J., 2000, Pb diffusion in rutile: Contributions to Mineralogy and Petrology, v. 139, p. 198–207, https://doi.org/10.1007/PL00007671.

Cherniak, D.J., Manchester, J., Watson, E.B., 2007, Zr and Hf diffusion in rutile: Earth and Planetary Science Letters, v. 261, p. 267–279, https://doi.org/10.1016/j.epsl.2007.06.027.

Chopin, C., 1984, Coesite and pure pyrope in high-grade blueschists of the Western Alps: A first record and some consequences: Contributions to Mineralogy and Petrology, v. 86, p. 107–118, https://doi.org/10.1007/BF00381838.

Duchêne, S., Lardeaux, J.-M., and Albarède, F., 1997, Exhumation of eclogites: Insights from depth-time path analysis: Tectonophysics, v. 280, p. 125–140, https://doi.org/10.1016/S0040-1951(97)00143-1.

Ernst, W.G., Maruyama, S., and Wallis, S., 1997, Buoyancy-driven, rapid exhumation of ultrahigh-pressure metamorphosed continental crust: Proceedings of the National Academy of Sciences of the United States of America, v. 94, p. 9532–9537, https://doi.org/10.1073/pnas.94.18.9532.

Ewing, T.A., Hermann, J., and Rubatto, D., 2013, The robustness of the Zr-in-rutile and Ti-in-zircon thermometers during high-temperature metamorphism (Ivrea-Verbano Zone, northern Italy): Contributions to Mineralogy and Petrology, v. 165, p. 757–779, https://doi.org/10.1007/s00410-012-0834-5.

Ewing, T.A., Rubatto, D., Beltrando, M., and Hermann, J., 2015, Constraints on the thermal evolution of the Adriatic margin during Jurassic continental break-up: U-Pb dating of rutile from the Ivrea-Verbano Zone, Italy: Contributions to Mineralogy and Petrology, v. 169, 44, https://doi.org/10.1007/s00410-015-1135-6.

Ganade, C.E., Rubatto, D., Hermann, J., Cordani, U.G., Caby, R., and Basei, M.A.S., 2014, Ediacaran 2,500-km-long synchronous deep continental subduction in the West Gondwana Orogen: Nature Communications, v. 5, 5198, https://doi.org/10.1038/ncomms6198.

Ganade, C.E., Lanari, P., Rubatto, D., Hermann, J., Weinberg, R.F., Basei, M.A.S., Tesser, L.R., Caby, R., Agbossoumondé, Y., and Ribeiro, C.M., 2021, Magmatic flare-up causes crustal thickening at the transition from subduction to continental collision: Communications Earth & Environment, v. 2, 41, https://doi.org/10.1038/s43247-021-00103-z.

Halverson, G.P., Dudás, F.Ö., Maloof, A.C., and Bowring, S.A., 2007, Evolution of the $^{87}Sr/^{86}Sr$ composition of Neoproterozoic seawater: Palaeogeography, Palaeoclimatology, Palaeoecology, v. 256, p. 103–129, https://doi.org/10.1016/j.palaeo.2007.02.028.

Hermann, J., Rubatto, D., Korsakov, A., and Shatsky, V.S., 2001, Multiple zircon growth during fast exhumation of diamondiferous, deeply subducted continental crust (Kokchetav Massif, Kazakhstan): Contributions to Mineralogy and Petrology, v. 141, p. 66–82, https://doi.org/10.1007/s004100000218.

Jahn, B.-m., Caby, R., and Monie, P., 2001, The oldest UHP eclogites of the World: Age of UHP metamorphism, nature of protoliths and tectonic implications: Chemical Geology, v. 178, p. 143–158, https://doi.org/10.1016/S0009-2541(01)00264-9.

Kooijman, E., Mezger, K., and Berndt, J., 2010, Constraints on the U-Pb systematics of metamorphic rutile from in situ LA-ICP-MS analysis: Earth and Planetary Science Letters, v. 293, p. 321–330, https://doi.org/10.1016/j.epsl.2010.02.047.

Kylander-Clark, A.R.C., Hacker, B.R., and Mattinson, C.G., 2012, Size and exhumation rate of ultrahigh-pressure terranes linked to orogenic stage: Earth and Planetary Science Letters, v. 321–322, p. 115–120, https://doi.org/10.1016/j.epsl.2011.12.036.

Lanari, P., Vidal, O., De Andrade, V., Dubacq, B., Lewin, E., Grosch, E.G., and Schwartz, S., 2014, XMapTools: A MATLAB©-based program for electron microprobe X-ray image processing and geothermobarometry: Computers & Geosciences, v. 62, p. 227–240, https://doi.org/10.1016/j.cageo.2013.08.010.

Liégeois, J.P., and Black, R., 1987, Alkaline magmatism subsequent to collision in the Pan-African belt of the Adrar des Iforas (Mali), *in* Fitton, J.G., and Upton, B.G.J., eds., Alkaline Igneous Rocks: Geological Society, London, Special Publication 30, p. 381–401, https://doi.org/10.1144/GSL.SP.1987.030.01.18.

Parrish, R.R., Gough, S.J., Searle, M.P., and Waters, D.J., 2006, Plate velocity exhumation of ultrahigh-pressure eclogites in the Pakistan Himalaya: Geology, v. 34, p. 989–992, https://doi.org/10.1130/G22796A.1.

Reichelt, R., 1966, Métamorphisme et plissement dans le Gourma et leurs âges (République du Mali): Compte Rendu de l'Académie des Sciences de Paris, v. 263, p. 589–592.

Rubatto, D., 2002, Zircon trace element geochemistry: Partitioning with garnet and the link between U-Pb ages and metamorphism: Chemical Geology, v. 184, p. 123–138, https://doi.org/10.1016/S0009-2541(01)00355-2.

Rubatto, D., 2017, Zircon: The metamorphic mineral: Reviews in Mineralogy and Geochemistry, v. 83, p. 261–295, https://doi.org/10.2138/rmg.2017.83.9.

Rubatto, D., and Hermann, J., 2001, Exhumation as fast as subduction?: Geology, v. 29, p. 3–6, https://doi.org/10.1130/0091-7613(2001)029<0003:EAFAS>2.0.CO;2.

Smith, D.C., 1984, Coesite in clinopyroxene in the Caledonides and its implications for geodynamics: Nature, v. 310, p. 641–644, https://doi.org/10.1038/310641a0.

Squire, R.J., Campbell, I.H., Allen, C.M., and Wilson, C.J.L., 2006, Did the Transgondwanan Supermountain trigger the explosive radiation of animals on Earth?: Earth and Planetary Science Letters, v. 250, p. 116–133, https://doi.org/10.1016/j.epsl.2006.07.032.

Stern, R.J., 2018, The evolution of plate tectonics: Philosophical Transactions of the Royal Society A: Mathematical, Physical and Engineering Sciences, v. 376, https://doi.org/10.1098/rsta.2017.0406.

Sun, R.Y., Shen, J., Grasby, S.E., Zhang, J.W., Chen, J.S., Yang, C., and Yin, R.S., 2022, CO_2 buildup drove global warming, the Marinoan deglaciation, and the genesis of the Ediacaran cap carbonates: Precambrian Research, v. 383, 106891, https://doi.org/10.1016/j.precamres.2022.106891.

Warren, C.J., Beaumont, C., and Jamieson, R.A., 2008, Formation and exhumation of ultra-high-pressure rocks during continental collision: Role of detachment in the subduction channel: Geochemistry, Geophysics, Geosystems, v. 9, Q04019, https://doi.org/10.1029/2007GC001839.

Watson, E.B., Wark, D.A., and Thomas, J.B., 2006, Crystallization thermometers for zircon and rutile: Contributions to Mineralogy and Petrology, v. 151, p. 413–433, https://doi.org/10.1007/s00410-006-0068-5.

Yan, L.L., and Zhang, K.J., 2019, Is exhumation of UHP terranes limited to low latitudes?: Journal of Geodynamics, v. 130, p. 41–56, https://doi.org/10.1016/j.jog.2019.06.004.

Printed in USA